

Protein Science

Solution structure of a small protein containing a fluorinated side chain in the core

Gabriel Cornilescu, Erik B. Hadley, Matthew G. Woll, John L. Markley, Samuel H. Gellman and Claudia C. Cornilescu

Protein Sci. 2007 16: 14-19; originally published online Nov 22, 2006;
Access the most recent version at doi:[10.1110/ps.062557707](https://doi.org/10.1110/ps.062557707)

References This article cites 33 articles, 2 of which can be accessed free at:
<http://www.proteinscience.org/cgi/content/full/16/1/14#References>

Email alerting service Receive free email alerts when new articles cite this article - sign up in the box at the top right corner of the article or [click here](#)

Correction A correction has been published for this article. The contents of the [correction](#) have been appended to the original article in this reprint. The correction is also available online at:
<http://www.proteinscience.org/cgi/content/full/protsci;16/9/2089>

Notes

To subscribe to *Protein Science* go to:
<http://www.proteinscience.org/subscriptions/>

Solution structure of a small protein containing a fluorinated side chain in the core

GABRIEL CORNILESCU,¹ ERIK B. HADLEY,² MATTHEW G. WOLL,²
JOHN L. MARKLEY,¹ SAMUEL H. GELLMAN,² AND CLAUDIA C. CORNILESCU¹

¹NMRFAM, Department of Biochemistry, University of Wisconsin, Madison, Wisconsin 53706, USA

²Department of Chemistry, University of Wisconsin, Madison, Wisconsin 53706, USA

(RECEIVED September 13, 2006; FINAL REVISION October 6, 2006; ACCEPTED October 10, 2006)

Abstract

We report the first high-resolution structure for a protein containing a fluorinated side chain. Recently we carried out a systematic evaluation of phenylalanine to pentafluorophenylalanine (Phe → F₅-Phe) mutants for the 35-residue chicken villin headpiece subdomain (c-VHP), the hydrophobic core of which features a cluster of three Phe side chains (residues 6, 10, and 17). Phe → F₅-Phe mutations are interesting because aryl–perfluoroaryl interactions of optimal geometry are intrinsically more favorable than either aryl–aryl or perfluoroaryl–perfluoroaryl interactions, and because perfluoroaryl units are more hydrophobic than are analogous aryl units. Only one mutation, Phe10 → F₅-Phe, was found to provide enhanced tertiary structural stability relative to the native core (by ~1 kcal/mol, according to guanidinium chloride denaturation studies). The NMR structure of this mutant, described here, reveals very little variation in backbone conformation or side chain packing relative to the wild type. Thus, although Phe → F₅-Phe mutations offer the possibility of greater tertiary structural stability from side chain–side chain attraction and/or side chain desolvation, the constraints associated with the native c-VHP fold apparently prevent the modified polypeptide from taking advantage of this possibility. Our findings are important because they complement several studies that have shown that fluorination of saturated side chain carbon atoms can provide enhanced conformational stability.

Keywords: pentafluorophenylalanine; backbone thioester exchange; villin headpiece; NMR; ¹H/¹⁹F and ¹⁹F/¹H heteronuclear NOE

Proteins are biochemical workhorses, performing a wide range of tasks that are essential for life. A remarkable breadth of activity is achieved by varying the sequential arrangement of a relatively small number of α-amino acid building blocks (~20), i.e., a relatively small number of side chain functionalities. Advances in genetic manipulation and heterologous expression have enabled the practical use of engineered proteins as medicines, industrial agents, and research tools, but the composition of manufactured non-natural proteins has to date been limited largely to the proteinogenic building blocks because of

constraints associated with the biosynthetic machinery. Incorporation of non-proteinogenic side chains can substantially expand the range of protein properties and functions (Wang and Schultz 2005), and the development of new strategies for protein synthesis promises to provide large-scale access to polypeptides containing non-proteinogenic subunits in the near future (Dawson and Kent 2000; Muir 2003; Wang and Schultz 2005). This prospect creates a need for fundamental knowledge regarding the effects of replacing natural side chains with non-proteinogenic analogs on the structure and other properties of folded proteins.

Fluorinated side chains have emerged as particularly interesting protein engineering tools (Marsh 2000; Yoder and Kumar 2002; Jäckel and Kokschi 2005), because replacement of C–H bonds with C–F bonds causes only a modest change in molecular volume but can induce

Reprint requests to: Claudia C. Cornilescu, NMRFAM, Department of Biochemistry, University of Wisconsin, Madison, WI 53706, USA; e-mail: cclaudia@nmrfam.wisc.edu; fax: (608) 262-3759.

Article published online ahead of print. Article and publication date are at <http://www.proteinscience.org/cgi/doi/10.1110/ps.062557707>.

dramatic changes in molecular interactions (Smart 2001; Dunitz 2004; Lai and Kool 2004). For example, saturated hydrocarbons and their perfluorocarbon analogs are immiscible, which indicates a strong preference for homointeraction over heterointeraction. Benzene and hexafluorobenzene, on the other hand, interact very favorably with one another; the 1:1 mixture has a higher melting point than does either pure substance (Williams 1993). The favorability of the C_6H_6/C_6F_6 interaction apparently reflects attractive quadrupolar interactions (West et al. 1997), among other factors, since adjacent C_6H_6 and C_6F_6 molecules stack face-to-face in the mixed solid, while such face-to-face interactions are absent in either pure solid. Both saturated and aliphatic fluorocarbon units are more hydrophobic than their hydrocarbon analogs, which represents an additional potential source of protein conformational stabilization (Smart 2001; Dunitz 2004; Lai and Kool 2004). On the other hand, replacing H with F results in a small increase in molecular volume, which could lead to steric repulsions in the folded state. Incorporation of fluorinated residues into polypeptides has usually resulted in conformational stabilization (Holmgren et al. 1998; Dawson and Kent 2000; Bilgicer et al. 2001; Tang et al. 2001; Butterfield et al. 2002; Muir 2003; Lee et al. 2004, 2006; Wang and Schultz 2005; Jäckel et al. 2006); however, most efforts to date have focused on fluorination of saturated carbon atoms, and the impact of aromatic fluorination has received little attention (Butterfield et al. 2002). None of the prior studies has provided high-resolution structural characterization of folded fluorine-containing polypeptides.

We recently undertook a systematic evaluation of phenylalanine-to-pentafluorophenylalanine (Phe \rightarrow F₅-Phe) mutants (M.G. Woll, E.B. Hadley, S. Mecozzi, and S.H. Gellman, in prep.), for the 35-residue chicken villin headpiece subdomain (c-VHP) (McKnight et al. 1997; Vardar et al. 1999; Vermeulen et al. 2004; Chiu et al. 2005), the hydrophobic core of which features a cluster of three Phe side chains (residues 6, 10, and 17). Of the seven possible F₅-Phe replacement patterns at the core positions, only Phe10 \rightarrow F₅-Phe was found to confer enhanced tertiary structural stability relative to the all-Phe core. Here we describe the solution structure of the stabilized F₅-Phe-containing cVHP mutant, based on NMR analysis. In addition to the Phe10 \rightarrow F₅-Phe mutation, all five of the lysine residues in cVHP were conservatively mutated to arginine (Fig. 1). Global replacement of the Lys residues in cVHP with Arg was required for implementation of a new method that we used to compare mutant conformational stabilities; stabilization of the tertiary structure by the Phe10 \rightarrow F₅-Phe mutation was demonstrated in the context of the Lys \rightarrow Arg replacements (M.G. Woll, E.B. Hadley, S. Mecozzi, and S.H. Gellman, in prep.). The structural results described here provide the first high-resolution

```

              10      20      30
cVHP  LSDEDFKAVF  GMTRSAFANL  PLWKQQLNKK  EKGLF
15F-cVHP LSDEDFRAV15F  GMTRSAFANL  PLWRQQLRR  ERGLF

```

Figure 1. Sequence comparison for cVHP and the F₅-Phe-containing mutant. For the latter sequence, residues indicated with bold letters represent points of divergence from the wild type (cVHP).

structural information on the packing of a fluorinated side chain within a folded protein.

Results

Resonance assignments and secondary structure

Assignments were made for ~90% of the backbone and side chains using PIPP/STAPP software (Garrett et al. 1991). The TALOS program (Cornilescu et al. 1999) used chemical shifts and sequence information to provide 29 pairs of ϕ/ψ backbone torsion angle restraints and to identify the secondary structure elements, confirmed by the NOE patterns characteristic of α -helical secondary structure (Fig. 2). Distance restraints of 1.9 Å and 2.9 Å were used to represent the H^N-O and N-O non-bonded distances, respectively, for the 12 inferred helical hydrogen bonds (Wüthrich 1986). Peak intensities from the NOE experiments were translated into a continuous distribution of interproton distance restraints, with a 40% distance uncertainty applied to take into account spin diffusion.

¹H/¹⁹F and ¹⁹F/¹H heteronuclear NOE (¹⁹F-HOESY) measurements with a 400-msec mixing time were used to obtain constraints for the F₅-Phe residue (spectra with 140 msec and 240 msec mixing times were also recorded but showed less or weaker peaks). All (¹⁹F-HOESY) spectra were acquired on a 500 MHz Bruker QNP probe (>90% of the peaks were assigned). Cross-peak intensities were divided

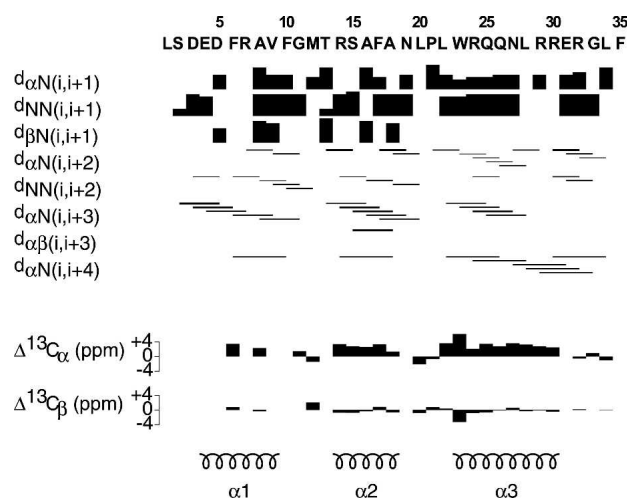


Figure 2. Summary of secondary structure elements; local NOE connectivities vs. the amino acid sequence of the F₅-Phe-containing mutant of cVHP.

into four bins, and the corresponding distance constraints were assigned proportionally to the ^1H NOEs (strongest and weakest intensities corresponded to 2.0 Å and 5.0 Å, respectively).

Our attempts to measure residual dipolar couplings (RDCs) resulted in either no quadrupolar splitting of the water signal due to interaction with the aligning medium for liquid crystalline positively charged bicelles (DMPC:DHPC:CTAB, 15:5:1; 5% w/v) (Ramirez and Bax 1998) or in unfolding of the peptide in 5% w/v C_{12}E_5 polyethylene glycol (PEG)/hexanol mixture with a surfactant to alcohol ratio of 0.96 (Ruckert and Otting 2000) and Helfrich lamellar phase, i.e., 5% w/v cetylpyridinium bromide (CPBr)/*n*-hexanol (Barrientos et al. 2000).

Structure determination

Simulated annealing, based on the described structural restraints, was carried out using the torsion angle molecular dynamics and the internal variable dynamics module (Schwieters and Clore 2001) of Xplor-NIH (Schwieters et al. 2003). Table 1 shows the structural statistics of the final structures. The target function minimized comprises the experimental NMR restraints (NOE-derived interproton distances and torsion angles), a repulsive van der Waals potential for the non-bonded contacts (Nilges et al. 1988), a torsion angle database potential of mean force (Clore and Kuszewski 2002), and a radius of gyration restraint (Kuszewski et al. 1999). The $^{19}\text{F}_5$ -Phe side chain topology and parameters were generated using The Dundee PRODRG2 Server (Schuettelkopf and van Aalten 2004).

To establish crucial contacts involving the F_5 -Phe side chain, we obtained 18 heteronuclear NOE restraints (seven of which were long-range) using 2D $^1\text{H}/^{19}\text{F}$ and $^{19}\text{F}/^1\text{H}$ heteronuclear NOE (^{19}F -HOESY) spectra. A total of 675 conventional NOE-derived interproton distance restraints (45 of which were long-range) were used for the structure calculations, along with the restraints mentioned above.

Superposition of the 20 lowest energy structures of the cVHP mutant is shown in Figure 3A. The tertiary fold consists of three α -helices connected by loops: helix $\alpha 1$ (residues 4–9), helix $\alpha 2$ (residues 14–18), and helix $\alpha 3$ (residues 23–30). The RMSD (residues 3–31) among the 20 lowest energy structures is 0.23 Å for the backbone atoms and 0.80 Å for all heavy atoms. The calculated structures show well-defined side chain conformations in the hydrophobic core of the protein. Broad rotameric restraints were derived from statistics of 100 structures calculated with torsion angle database potentials (Clore and Kuszewski 2002). More precisely, the energetically favorable rotameric combinations were deduced from the sterically allowed configurations in the cVHP fold in conjunction with statistics of the database of high

Table 1. Structural statistics

	$\langle S_a \rangle^a$	RMS deviations Lowest energy
Experimental ^1H - ^1H distance restraints (Å) (675)		
Intraresidue (323)	0.027 ± 0.002	0.028
Sequential $ i - j = 1$ (147)	0.072 ± 0.004	0.073
Short range $1 < i - j \leq 5$ (160)	0.083 ± 0.005	0.086
Long range $ i - j > 5$ (45)	0.074 ± 0.014	0.056
Experimental ^1H - ^{19}F distance restraints (Å) (18)		
Intraresidue (4)	0.000 ± 0.000	0.000
Sequential $ i - j = 1$ (4)	0.168 ± 0.028	0.164
Short range $1 < i - j \leq 5$ (3)	0.254 ± 0.018	0.255
Long range $ i - j > 5$ (7)	0.230 ± 0.039	0.233
Hydrogen bonds (Å) (12)	0.007 ± 0.008	0.012
Predicted dihedral restraints (°) (58)		
	0.624 ± 0.065	0.563
Deviations from idealized covalent geometry		
Bonds (Å) (593)	0.00143 ± 0.00004	0.00143
Angles (°) (1057)	0.279 ± 0.001	0.278
Impropers (°) (334)	0.571 ± 0.109	0.521
Measures of structure quality		
Lennard-Jones energy ^b (kcal/mol)		
	-362 ± 55	-413
Ramachandran analysis ^c		
Residues in most favored regions (%)	99.8	100
Residues in allowed regions (%)	0.2	0
Residues in disallowed regions (%)	0.0	0
Coordinate precision ^d		
Backbone (N, C $^\alpha$, C')	0.23 ± 0.10	
All non-hydrogen atoms	0.80 ± 0.09	

The statistics are for the 20 structures (of 100 calculated) with the overall lowest energies.

^a $\langle S_a \rangle$ represents the 20 lowest-energy structures. For $\langle S_a \rangle$, the values shown are mean ± standard deviation with the number of restraints used to calculate these values shown in parentheses.

^bThe van der Waals energies described by Lennard-Jones potentials were not incorporated into the simulated annealing calculation.

^cCalculated for residues 3–31.

^dAverage RMSD of the 20 lowest-energy structures from the mean coordinates for residues 3–31.

resolution structures used to derive those potentials. For example, the presence in more than 95% of the cVHP calculated structures of a $-60^\circ/180^\circ (\pm 30^\circ)$ Leu χ_1 can be used to constrain its χ_2 to $180^\circ/60^\circ (\pm 30^\circ)$, respectively. To eliminate any possible bias caused either by rotameric constraints or by ambiguities in the ^{19}F NOE assignments, we repeated the structure calculation with these constraints removed. The resulting structures did not show any major change in the conformations or packing of the core Phe residues 6, 10, and 17.

Discussion

The overall backbone fold is remarkably invariant among the several X-ray and NMR structures of VHP-family proteins solved to date (McKnight et al. 1997; Vardar

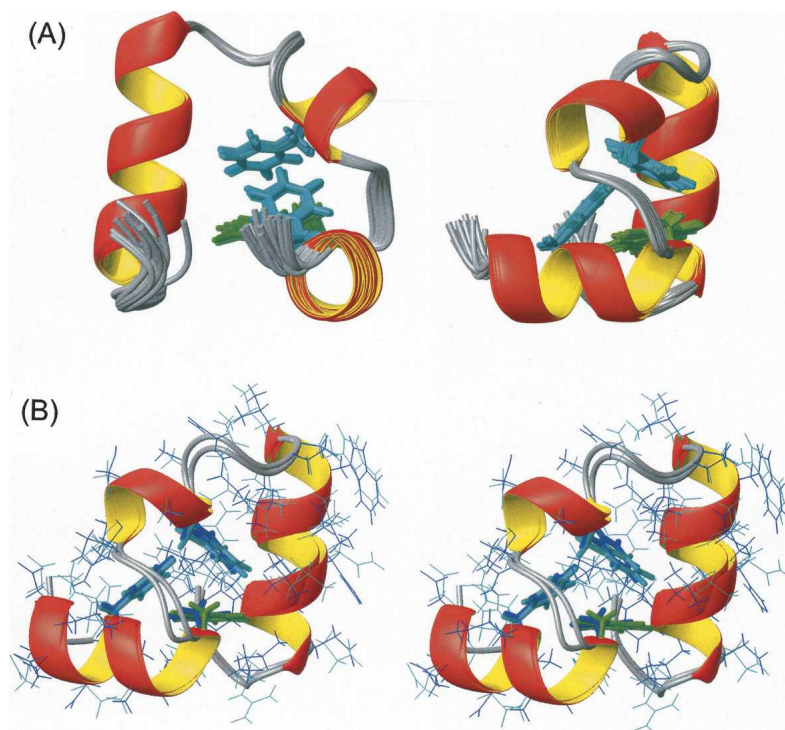


Figure 3. (A) Ensemble of the 20 lowest energy backbone structures of the F₅-Phe-containing mutant of cVHP, based on NMR (*left*). The same ensemble of structures rotated by (−90°) about the vertical axis (*right*). (B) Stereo view of best-fit superposition (RMSD = 0.66 Å) of the heavy backbone atoms (residues 3–31) of the NMR structure of the Phe10 → F₅-Phe variant of m-cVHP and the X-ray structure of the His27 → Asn mutant of cVHP (19). Side chains for the NMR structure are shown in thick green for F₅-Phe10, thick cyan for Phe6 and Phe17, or thin cyan for all others; side chains for X-ray structure shown in thick blue for Phe6, Phe10, and Phe17, or thin blue for all others.

et al. 1999; Vermeulen et al. 2004; Chiu et al. 2005), including ours. Best-fit superposition of the heavy backbone atoms from residues 3–31 of our structure with the corresponding residues from a recently published 1 Å-resolution X-ray structure (Chiu et al. 2005) results in an RMSD of 0.66 Å (Fig. 3B). The differences between the two sequences consist of the Phe10 → F₅-Phe mutation along with the five conservative Lys → Arg mutations in our version and a His27 → Asn mutation in the crystallized version (residue 27 is situated in the middle of helix α3 with its side chain pointing away from the hydrophobic core). The similarity between these two structures indicates that the five Lys → Arg mutations we made to facilitate the thermodynamic comparisons do not exert a significant effect on the VHP tertiary fold.

Since the atomic radius of fluorine is only 0.27 Å greater than that of hydrogen, replacement of hydrogen by fluorine is often regarded as an isosteric substitution. The effect of the extra steric bulk created by the Phe10 → F₅-Phe substitution appears to be minor compared to the more important changes in the electrostatic properties of the aromatic ring. Our structural data show that Phe10 → F₅-Phe mutation exerts very little effect on the cVHP

tertiary structure, even though fluorination of the Phe10 side chain stabilizes the cVHP fold by 1 kcal/mol, according to guanidinium chloride denaturation studies (M.G. Woll, E.B. Hadley, S. Mecozzi, and S.H. Gellman, in prep.). The similarity between the polypeptide conformations anchored by the Phe/Phe/Phe and Phe/F₅-Phe/Phe cores, and the diminution in conformational stability arising from all other Phe → F₅-Phe mutations suggest that the VHP fold has little capacity to realize the potential for improved side chain–side chain interactions provided by introduction of a fluoroaryl ring. We initially anticipated that a F₅-Phe-containing mutant might depart modestly from the native cVHP fold to gain stability from an energetically favorable face-to-face juxtaposition of Phe and F₅-Phe side chains; indeed, we suspected that the small size of this folding unit might make it particularly amenable to minor changes in side chain packing (fewer compensating changes required than in a larger folded domain). The structural results described here, however, suggest that such a conformational adjustment would entail an energetic cost that cannot be recouped from the Phe/F₅-Phe interaction itself. The enhanced conformational stability and native-like fold of the Phe10 → F₅-Phe mutant

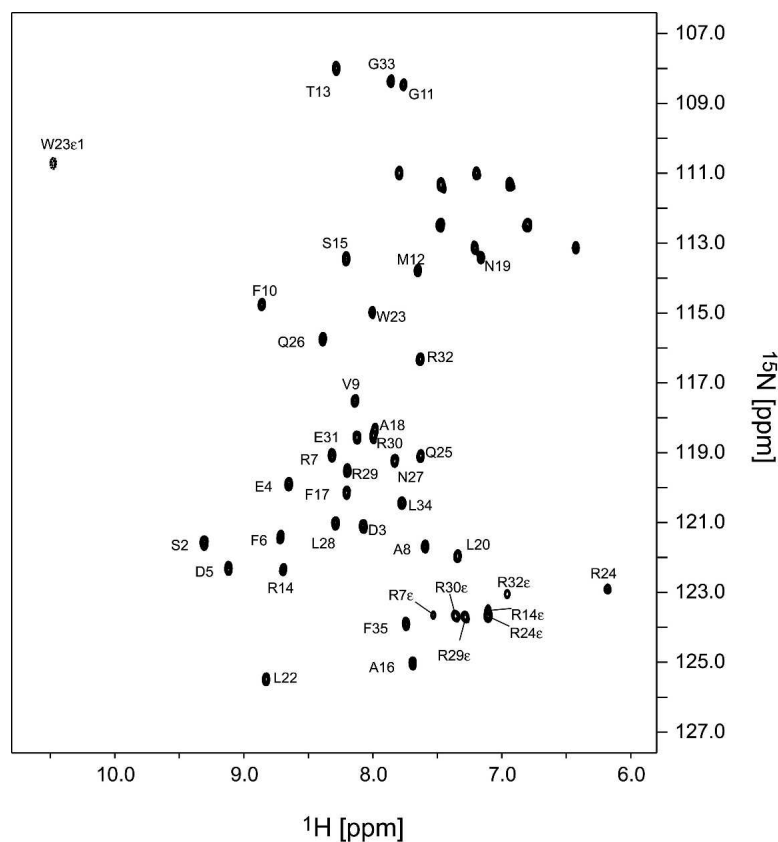


Figure 4. ^1H - ^{15}N HSQC of data for the F₅-Phe-containing mutant of cVHP (unlabeled sample).

suggest that conferring greater stability *by design* on cVHP, and perhaps other protein folding patterns, will require careful selection and positioning of side chains that can increase stability in the native tertiary context. It will be interesting to see whether the apparent resistance of the VHP tertiary structure to backbone rearrangement/core repacking in response to incorporation of non-natural side chains proves to be general. This prospect should influence other efforts to design folding units that contain non-proteinogenic side chains.

Materials and methods

Protein expression and purification

Peptides were synthesized on solid phase using a Synergy automated synthesizer (Applied Biosystems model 432A loaded with 9-fluorenylmethoxycarbonyl [Fmoc]-Phe-Wang polystyrene resin). Synthetic cycles were completed with a standard coupling time of 30 min using *O*-benzotriazol-1-yl-*N,N,N'*,*N'*-tetramethyluronium hexafluorophosphate (HBTU, four equivalents) and DMF as solvent. Three equivalents of Fmoc amino acid were used for each coupling cycle. Deprotection steps used 20% piperidine in DMF for 15 min. Peptides were cleaved and/or deprotected by stirring with (CF₃CO₂H:H₂O:triisopropylsilane, 90:5:5, v/v/v) (2 mL/25 μmol) for 4 h followed by precipitating

into cold diethyl ether. The precipitate was collected by centrifugation/decantation prior to purification. Peptides were purified by reverse-phase HPLC and characterized by analytical HPLC and matrix-assisted laser desorption ionization (MALDI) mass spectrometry.

Characterization data

m-cVHP

HPLC: C18 preparative column (25 × 250 mm), flow rate 15 mL/min, gradient of 30%–40% B solvent (CH₃CN:CF₃COOH, 100:0.1, v/v) in A (H₂O:CF₃CO₂H, 100:0.1, v/v) over 20 min, retention time of 17.2 min. MALDI-TOF [M + H]⁺ + calculated 4196.1, observed 4198.7.

m-cVHP (F10f₅-F)

HPLC: C18 preparative column (25 × 250 mm), flow rate 15 mL/min, gradient of 30%–40% B solvent (CH₃CN:CF₃COOH, 100:0.1, v/v) in A (H₂O:CF₃CO₂H, 100:0.1, v/v) over 20 min, retention time of 15.8 min. MALDI-TOF [M + H]⁺ + calculated 4286.1, observed 4287.1.

NMR measurements

NMR data were acquired at 25°C on 280 μL samples at pH 5.0 containing either 4.0 mM of unlabelled protein or 2 mM of selectively ^{15}N -[Ala, Phe, Leu]-labeled protein, 10 mM sodium

phosphate, and 0.1 mM Na₂N₃ in either 93% H₂O/7% ²H₂O or 99.9% ²H₂O. [¹H-¹⁵N] HSQC, [¹H-¹³C] HSQC, COSY, TOCSY, and 2D NOESY (*t*_{mix} = 140 msec) spectra were collected on the unlabeled sample. Significant resonance overlap, as expected for a largely α -helical protein, allowed assignment of only ~40% of the proton resonances for the unlabeled sample (Fig. 4). [¹H-¹⁵N] HSQC, 2D HNCACB, 2D HNCO, 3D HNHA, and 3D HNHB spectra were acquired on the selectively ¹⁵N-[Ala, Phe, Leu]-labeled sample. NMR experiments were performed on Varian INOVA 600 and 900 MHz, Bruker AVANCE 500 and 600 MHz spectrometers. Varian INOVA 600 MHz and Bruker AVANCE 600 MHz were equipped with cryogenic probes. NMR data were processed using the NMRPipe package (Delaglio et al. 1995).

Accession numbers

Coordinates have been deposited at the Protein Data Bank (PDB ID 2JM0) and NMR data at BMRB (accession no. 15000).

Acknowledgments

We thank Charles Schwieters and Marius Clore for helpful suggestions on incorporating F₅-Phe into the XPLOR-NIH analysis; Prof. C.J. McKnight for providing NMR coordinates in advance of publication; and Charles G. Fry, Mark E. Anderson, Ed S. Mooberry, and William M. Westler for helpful discussions on ¹⁹F heteronuclear NOE. This research was supported in part by NIH grant R01 GM-61238 (S.H.G.). M.G.W. was the recipient of a fellowship from the Organic Division of the American Chemical Society, supported by Eli Lilly and Company. This study made use of the National Magnetic Resonance Facility at Madison, which is supported by NIH grants P41RR02301 (Biomedical Research Technology Program, NCRR) and P41GM66326 (NIGMS). Equipment in the facility was purchased with funds from the University of Wisconsin, the NIH (P41GM66326, P41RR02301, RR02781, RR08438), the NSF (DMB-8415048, OIA-9977486, BIR-9214394), and the USDA.

References

Barrientos, L.G., Dolan, C., and Gronenborn, A.M. 2000. Characterization of surfactant liquid crystal phases suitable for molecular alignment and measurement of dipolar couplings. *J. Biomol. NMR* **16**: 329–337.

Bilgicer, B., Fichera, A., and Kumar, K. 2001. A coiled coil with a fluororous core. *J. Am. Chem. Soc.* **123**: 4393–4399.

Butterfield, S.M., Patel, P.R., and Waters, M.L. 2002. Contribution of aromatic interactions to α -helix stability. *J. Am. Chem. Soc.* **124**: 9751–9755.

Chiu, T.K., Kubelka, J., Herbst-Irmer, R., Eaton, W.A., Hofrichter, J., and Davies, D.R. 2005. High-resolution x-ray crystal structures of the villin headpiece subdomain, an ultrafast folding protein. *Proc. Natl. Acad. Sci.* **102**: 7517–7522.

Clore, G.M. and Kuszewski, J. 2002. χ_1 rotamer populations and angles of mobile surface side chains are accurately predicted by a torsion angle database potential of mean force. *J. Am. Chem. Soc.* **124**: 2866–2867.

Cornilescu, G., Delaglio, F., and Bax, A. 1999. Protein backbone angle restraints from searching a database for chemical shift and sequence homology. *J. Biomol. NMR* **13**: 289–302.

Dawson, P.E. and Kent, S.B.H. 2000. Synthesis of native proteins by chemical ligation. *Annu. Rev. Biochem.* **69**: 923–960.

Delaglio, F., Grzesiek, S., Vuister, G.W., Zhu, G., Pfeifer, J., and Bax, A. 1995. NMRPIPE—A multidimensional spectral processing system based on UNIX pipes. *J. Biomol. NMR* **6**: 277–293.

Dunitz, J.D. 2004. Organic fluorine: Odd man out. *ChemBioChem* **5**: 614–621.

Garrett, D.S., Powers, R., Gronenborn, A.M., and Clore, G.M. 1991. A common-sense approach to peak picking in 2-dimensional, 3-dimensional, and 4-dimensional spectra using automatic computer-analysis of contour diagrams. *J. Magn. Reson.* **95**: 214–220.

Holmgren, S.K., Taylor, K.M., Bretscher, L.E., and Raines, R.T. 1998. Code for collagen's stability deciphered. *Nature* **392**: 666–667.

Jäckel, C. and Koksche, B. 2005. Fluorine in peptide design and protein engineering. *Eur. J. Org. Chem.* **21**: 4483–4503.

Jäckel, C., Salwiczek, M., and Koksche, B. 2006. Fluorine in a native protein environment—How the spatial demand and polarity of fluoroalkyl groups affect protein folding. *Angew. Chem. Int. Ed. Engl.* **45**: 4198–4203.

Kuszewski, J., Gronenborn, A.M., and Clore, G.M. 1999. Improving the packing and accuracy of NMR structures with a pseudopotential for the radius of gyration. *J. Am. Chem. Soc.* **121**: 2337–2338.

Lai, J.S. and Kool, E.T. 2004. Selective pairing of polyfluorinated DNA bases. *J. Am. Chem. Soc.* **126**: 3040–3041.

Lee, K.-H., Lee, H.-Y., Slutsky, M.M., Anderson, J.T., and Marsh, E.N.G. 2004. Fluorous effect in proteins: De novo design and characterization of a four- α -helix bundle protein containing hexafluorooleucine. *Biochemistry* **43**: 16277–16284.

Lee, H.-Y., Lee, K.-H., Al-Hashimi, H.M., and Marsh, E.N.G. 2006. Modulating protein structure with fluororous amino acids: Increased stability and native-like structure conferred on a 4-helix bundle protein by hexafluorooleucine. *J. Am. Chem. Soc.* **128**: 337–343.

Marsh, E.N.G. 2000. Towards the nonstick egg: Designing fluororous proteins. *Chem. Biol.* **7**: R153–R157.

McKnight, C.J., Matsudaira, P.T., and Kim, P.S. 1997. NMR structure of the 35-residue villin headpiece subdomain. *Nat. Struct. Biol.* **4**: 180–184.

Muir, T.W. 2003. Semisynthesis of proteins by expressed protein ligation. *Annu. Rev. Biochem.* **72**: 249–289.

Nilges, M., Clore, G.M., and Gronenborn, A.M. 1988. Determination of three-dimensional structures of proteins from interproton distance data by hybrid distance geometry-dynamical simulated annealing calculations. *FEBS Lett.* **229**: 317–324.

Ramirez, B.E. and Bax, A. 1998. Modulation of the alignment tensor of macromolecules dissolved in a dilute liquid crystalline medium. *J. Am. Chem. Soc.* **120**: 9106–9107.

Ruckert, M. and Otting, G. 2000. Alignment of biological macromolecules in novel nonionic liquid crystalline media for NMR experiments. *J. Am. Chem. Soc.* **122**: 7793–7797.

Schuettelkopf, A.W. and van Aalten, D.F.M. 2004. PRODRG: A tool for high-throughput crystallography of protein-ligand complexes. *Acta Crystallogr. D Biol. Crystallogr.* **60**: 1355–1363.

Schwieters, C.D. and Clore, G.M. 2001. Internal coordinates for molecular dynamics and minimization in structure determination and refinement. *J. Magn. Reson.* **152**: 288–302.

Schwieters, C.D., Kuszewski, J.J., Tjandra, N., and Clore, G.M. 2003. The Xplor-NIH NMR molecular structure determination package. *J. Magn. Reson.* **160**: 65–73.

Smart, B.E. 2001. Fluorine substituent effects (on bioactivity). *J. Fluor. Chem.* **109**: 3–11.

Tang, Y., Ghirlanda, G., Vaidehi, N., Kua, J., Mainz, D.T., Goddard, W.A., DeGrado, W.F., and Tirrell, D.A. 2001. Stabilization of coiled-coil peptide domains by introduction of trifluorooleucine. *Biochemistry* **40**: 2790–2796.

Vardar, D., Buckley, D.A., Frank, B.S., and McKnight, C.J. 1999. NMR structure of an F-actin-binding “headpiece” motif from villin. *J. Mol. Biol.* **294**: 1299–1310.

Vermeeulen, W., Vanhaesebrouck, P., Van Troys, M., Verschueren, M., Fant, F., Goethals, M., Ampe, C., Martins, J.C., and Borremans, F.A.M. 2004. Solution structures of the C-terminal headpiece subdomains of human villin and advillin, evaluation of headpiece F-actin-binding requirements. *Protein Sci.* **13**: 1276–1287.

Wang, L. and Schultz, P.G. 2005. Expanding the genetic code. *Angew. Chem. Int. Ed. Engl.* **44**: 34–66.

West, A.P., Mecozzi, S., and Dougherty, D.A. 1997. Theoretical studies of the supramolecular synthon benzene- \cdots hexafluorobenzene. *J. Phys. Org. Chem.* **10**: 347–350.

Williams, J.R. 1993. The molecular electric quadrupole moment and solid-state architecture. *Acc. Chem. Res.* **26**: 593–598.

Wüthrich, K. 1986. *NMR of proteins and nucleic acids*. Wiley Interscience, New York.

Yoder, N.C. and Kumar, K. 2002. Fluorinated amino acids in protein design and engineering. *Chem. Soc. Rev.* **31**: 335–341.

CORRECTION

Protein Science **16**: 14–19 (2007)

Solution structure of a small protein containing a fluorinated side chain in the core

Gabriel Cornilescu, Erik B. Hadley, Matthew G. Woll, John L. Markley, Samuel H. Gellman, and Claudia C. Cornilescu

We, the authors, retract the claim that the structure reported is the first to include a fluorinated side chain. A number of prior structures that contain side chains bearing a single H → F substitution have been reported, and we regret not having cited these (Ji et al. 1994, 1997; Xiao et al. 1998; Minks et al. 1999; Rozovsky et al. 2001; Campos-Olivas et al. 2002; Alexeev et al. 2003; Bae et al. 2004; Ayala et al. 2005; Wang et al. 2005). To our knowledge, however, ours is the first report of a protein structure containing a more heavily fluorinated side chain (bearing at least three F atoms), for which non-negligible structural rearrangements may be expected.

References

- Alexeev, D., Barlow, P.N., Bury, S.M., Charrier, J.D., Cooper, A., Hadfield, D., Jamieson, C., Kelly, S.M., Layfield, R., Mayer, R.J., et al. 2003. Synthesis, structural and biological studies of ubiquitin mutants containing (2S, 4S)-5-fluoroleucine residues strategically placed in the hydrophobic core. *ChemBiochem*. **4**: 894–896.
- Ayala, I., Perry, J.J., Szczepanski, J., Tainer, J.A., Vala, M.T., Nick, H.S., and Silverman, D.N. 2005. Hydrogen bonding in human manganese superoxide dismutase containing 3-fluorotyrosine. *Biophys. J.* **89**: 4171–4179.
- Bae, J.H., Pal, P.P., Moroder, L., Huber, R., and Budisa, N. 2004. Crystallographic evidence for isomeric chromophores in 3-fluorotyrosyl-green fluorescent protein. *ChemBiochem*. **5**: 720–722.
- Campos-Olivas, R., Aziz, R., Helms, G.L., Evans, J.N.S., and Gronenborn, A.M. 2002. Placement of 19F into the center of GB1: Effects on structure and stability. *FEBS Letters* **517**: 55–60.
- Ji, X.H., Johnson, W.W., Sesay, M.A., Dickert, L., Prasad, S.M., Ammon, H.L., Armstrong, R.N., and Gilliland, G.L. 1994. Structure and function of the xenobiotic substrate-binding site of A glutathione-S-transferase as revealed by X-ray crystallographic analysis of product complexes with diastereomers of 9-(S-glutathionyl)-10-hydroxy-9,10-dihydrophenanthrene. *Biochem.* **33**: 1043–1052.
- Ji, X.H., Tordova, M., O'Donnell, R., Parsons, J.F., Hayden, J.B., Gilliland, G.L., and Zimniak, P. 1997. Structure and function of the xenobiotic substrate-binding site and location of a potential non-substrate-binding site in a class pi glutathione S-transferase. *Biochem.* **36**: 9690–9702.
- Minks, C., Huber, R., Moroder, L., and Budisa, N. 1999. Atomic mutations at the single tryptophan residue of human recombinant annexin V: Effects on structure, stability, and activity. *Biochem.* **38**: 10649–10659.
- Rozovsky, S., Jogl, G., Tong, L., and McDermott, A.E. 2001. Solution-state NMR investigations of triosephosphate isomerase active site loop motion: Ligand release in relation to active site loop dynamics. *J. Mol. Biol.* **310**: 271–280.
- Wang, X., Mercier, P., Letourneau, P.J., and Sykes, B.D. 2005. Effects of Phe-to-Trp mutation and fluorotryptophan incorporation on the solution structure of cardiac troponin C, and analysis of its suitability as a potential probe for in situ NMR studies. *Protein Sci.* **14**: 2447–2460.
- Xiao, G.Y., Parsons, J.F., Tesh, K., Armstrong, R.N., and Gilliland, G.L. 1998. Conformational changes in the crystal structure of rat glutathione transferase M1-1 with global substitution of 3-fluorotyrosine for tyrosine. *J. Mol. Biol.* **281**: 323–339.